Human CC Chemokine I-309, Structural Consequences of the Additional Disulfide Bond[†,‡]

David W. Keizer,[§] Matthew P. Crump,[||] Tae Woo Lee,[§] Carolyn M. Slupsky,[§] Ian Clark-Lewis,[⊥] and Brian D. Sykes*[,§]

Protein Engineering Network Centres of Excellence (PENCE) and Department of Biochemistry, 713 Heritage Medical Research Centre, University of Alberta, Edmonton, Alberta, Canada T6G 2S2, Department of Biochemistry, University of Southampton, Bassett Crescent East, Southampton SO16 7PX, U.K., and Biomedical Research Centre and Department of Biochemistry and Molecular Biology, University of British Columbia, Vancouver, British Columbia, Canada V6T 1Z3

Received January 14, 2000; Revised Manuscript Received March 21, 2000

ABSTRACT: I-309 is a member of the CC subclass of chemokines and is one of only three human chemokines known to contain an additional, third disulfide bond. The three-dimensional solution structure of I-309 was determined by ^{1}H nuclear magnetic resonance spectroscopy and dynamic simulated annealing. The structure of I-309, which remains monomeric at high concentrations, was determined on the basis of 978 experimental restraints. The N-terminal region of I-309 was disordered, as has been previously observed for the CC chemokine eotaxin but not others such as MCP-1 and RANTES. This was followed in I-309 by a well-ordered region between residues 13 and 69 that consisted of a 3_{10}-helix, a triple-stranded antiparallel β-sheet, and finally a C-terminal α-helix. Root-mean-square deviations of 0.61 and 1.16 were observed for the backbone and heavy atoms, respectively. A comparison of I-309 to eotaxin and HCC-2 revealed a significant structural change in the C-terminal region of the protein. The α-helix normally present in chemokines was terminated early and was followed by a short section of extended strand. These changes were a direct result of the additional disulfide bond present in this protein. An examination of the I-309 structure will aid in an understanding of the specificity of this protein with its receptor, CCR8.

The chemotactic cytokines (chemokines) and their cognate receptors are a superfamily of proteins that are essential in orchestrating leukocyte chemotaxis and host inflammatory responses (*1*). Chemokines are small proteins (66−80 amino acids) that tend to be highly conserved across species (i.e., an average degree of identity of 69% between human and mouse) and can even be almost identical (SDF-1; *2*). This pattern of conservation has suggested other fundamental developmental roles outside of the immune response (*3*). The family is divided into two major classes, CC and CXC, dependent upon the location of two highly conserved N-terminal cysteine residues (adjacent and separated by an intervening residue, respectively; *4, 5*) that are involved in the formation of a pair of disulfide bonds. Increasingly, however, chemokines are being discovered that lie outside this classification, and a number of subclasses are required to group these newer members (e.g., fractalkine, CX_3C; lymphotactin, C). I-309 is a member of a subclass that contains three disulfide bonds: two in a CC arrangement at the N-terminus and a third that is well-separated in the sequence from this motif (*6*). Two other chemokines, HCC-2[1] and Ckβ8, have been found to contain an additional disulfide bond (*7*, *8*), although the location of the third disulfide bond appears to be variable. Chemokines stimulate a wide variety of cell types and initiate signal transduction at the plasma membrane of cells via G-protein-coupled seven-transmembrane receptors (*9*). Recruitment of given leukocyte populations is dictated by a combination of a chemokine's receptor specificity and cell distribution of that receptor (*10, 11*). I-309 has been shown to be specific for CCR8 (*12, 13*), where it displays a potency similar to that of other chemokines for their receptors (threshold for calcium flux response of 0.1 nM). CCR8 transcripts are not expressed in lymphocytes or neutrophils (*14*) and, contrary to some reports, are not expressed in monocytes (*12*). Conversely, CCR8 has been shown to be specific for I-309 while insensitive to 20 other chemokines (*13*).[2] The tissue expression of CCR8 is unique, with constitutive mRNA expression

[†] Project funded by the Protein Engineering Network Centres of Excellence.

[‡] The atomic coordinates of the minimized average structure, the family of 40 structures, and restraint files have been deposited in The RCSB Protein Data Bank, with access code 1EL0. Chemical shifts have been deposited in the BioMagResBank with access code 4686.

* To whom correspondence should be addressed. Phone: (780) 492-6540. Fax: (780) 492-1473. E-mail: brian.sykes@ualberta.ca.

[§] University of Alberta.

[||] University of Southampton.

[⊥] University of British Columbia.

[1] Abbreviations: CCR, CC chemokine receptor; DSS, 2,2-dimethyl-2-silapentane-5-sulfonic acid; DQF-COSY, double-quantum-filtered correlated spectroscopy; HCC-2, human CC chemokine 2; HIV-1, human immunodeficiency virus type 1; HSQC, heteronuclear single-quantum coherence; MCP, monocyte chemoattractant protein; MIP, macrophage inflammatory protein; NMR, nuclear magnetic resonance; NOESY, nuclear Overhauser enhancement spectroscopy; RANTES, regulated upon activation, T-cell expressed, and secreted; rmsd, root-mean-square deviation; TOCSY, total correlation spectroscopy.

[2] TARC and MIP-1β have been reported as ligands for CCR8 (*15*), but this finding has since been contested (*16*).

10.1021/bi000089l CCC: $19.00
Published on Web 04/26/2000

```
         1          10         20         30          40          50        60        70
I-309    SKSMQVP  FSR CCFSFAEQEIPLRAILCYRNTSSI CSNEG LIFKLKRGKE  ACALDTVQWVQRHRKMLRHCPS  KRK
TCA3     SKMLTVS  NS  CCLNTLKKELPLKFIQCYRKMGSS CPDPPAVVFRLNKGRE  SCASTNKTWVQNHLKKVNPC
Eotaxin   GPASVP   TT CCFNLANRKIPLQRLESYRRITSGKCPQK AVIFKTKLAKD  ICADPKKKWVQDSMKYLDQKSP  TPKP
HCC-2          H  FAADCCTSYISQSIPCSLMKSYFE TSSECSKP GVIFLTKKGRQ  VCAKPSGPGVQDCMKKLKPYSI
MCP-3     QPVGIN  TSTTCCYRFINKKIPKQRLESYRRTTSSHCPRE AVIFKTKLDKE  ICADPTQKWVQDFMKHLDKKTQ  TPKL
MCP-1     QPDAIN  APVTCCYNFTNRKISVQRLASYRRITSSKCPKE AVIFKTIVAKE  ICADPKQKWVQDSMDHLDKQTQ  TPKT
vMIPI    AGSLVSY  TPNSCCYGFQQHPPPVQILKEWYP TSPACPKPG VILLTKRGRQ  ICADPSKNWVRQLMQRLPAIA
MIP-1β    APMGSD  PPTACCFSYTARKLPRNFVVDYYETSS  CSQP AVVFQTKRSKQ  VCADPSESWVQEYVYDLELN
vMIPII      LGASWHRPDKCCLGYQKRPLP QVLLSSWYPTSQLCSKPG VIFLTKRGRQ  VCADKSKDWVKKLMQQLPVTAR
CKβ8        MDRFHATSADCCISYTPRSIPCSLLESYFETNS ECSKPG VIFLTKKGRRRFFCANPSDKQVQVCMRMLKLDTRIKTRKN
RANTES       SPYSSDTTPCCFAYIARPLPRAHIKEYFY TSGKCSNP AVVFVTRKNRQ  VCANPEKKWVREYINSLEMS
Summary  -------------CC--------P------Y----S--C-----V-F-TK-------CA-P---WVQ-----L-----------
```

FIGURE 1: Amino acid sequence of I-309 aligned with those of Ckβ8, eotaxin, HCC-2, MCP-1, MCP-3, MIP-I, MIP-1β, MIP-II, RANTES, TCA-3, vMIP-I, and vMIP-II. Sequences are numbered according to I-309 and shown in order of decreasing degree of identity with I-309. The alignment was produced using XALIGN (*61*).

occurring in the thymus, while other chemokine receptors may be expressed in many tissues. This confers I-309 with the ability of blocking dexamethasone-induced apoptosis in mouse thymic cell lines and may infer a role for I-309 in thymocytic migration and development. This suggests the exciting possibility of a more fundamental role for the I-309−CCR8 coupling. The selectivity is unusual and has only been seen previously for CXCR1 and CXCR4 that bind IL-8 and SDF-1, respectively. Alongside I-309, only virally encoded chemokines exhibit a high affinity for the CCR8 receptor; HHV8 encoded vMIP-I and vMIP-II and MCV-encoded vMCC-1 (*17*, *18*). Whereas vMIP-II and vMCC-1 have promiscuous and antagonistic receptor binding profiles (*19*), vMIP-I, like I-309, is a specific agonist for CCR8. The functional relevance of vMIP-I, whose sequence is only 52% identical (Figure 1), mimicking I-309 function is unclear.

I-309 has been shown to inhibit CCR8-dependent cell−cell fusion and infection by a diverse range of HIV-1 strains (*20*). Macrophage tropic or non-syncitia-inducing strains of HIV-1 primarily use CCR5 (*21*), while syncitia-inducing, T-cell tropic strains that emerge in the progressed stages of infection primarily use CXCR4 (*22*). In addition, several additional receptors can act as coreceptors, e.g., CCR2b and CCR3 (*23*, *24*), and some dual-tropic strains can adopt several different receptors. CCR8, however, may contribute uniquely to the pathogenesis of HIV-1 as it has been identified as a coreceptor for several HIV-1 types, including macrophage, T-cell, and dual-tropic strains (*20*). I-309 is nevertheless able to block CCR8-mediated infection by these strains.

As the chemokine family and their receptors emerged with an increasingly complex array of subtypes and interactions, detailed structural and functional studies have attempted to separate purely structural regions within the chemokine fold from regions important for receptor specificity and/or receptor triggering. To date, the CXC chemokines IL-8 (*25*, *26*), PF4 (*20*, *27*), MGSA (*28*, *29*), CINC/Gro (*30*), SDF-1α (*31*, *32*), NAP-2 (*33*), MIP-2 (*34*), CC chemokines MIP-1β (*35*), RANTES (*36*, *37*), MCP-3 (*38*, *39*), MCP-1 (*40*, *41*), eotaxin (*42*), and the CX_3C chemokine fractalkine (*43*) structures have been determined by either NMR or X-ray crystallography. Structurally, these studies have revealed that the chemokine tertiary fold is remarkably homogeneous, being comprised of a central core of a three-stranded antiparallel β-sheet packed against a C-terminal α-helix. Preceding this core is an N-terminal region (typically 5−10 residues) and the N-loop (typically about 9 residues) that are anchored to the core via the twin disulfide bridges. Functional studies have revealed that varying patterns of residues within the N-terminus and N-loop have predominant control over receptor specificity and binding while selected residues within the core show at best only minor contributions. Historically, the first structures that were determined revealed differing quaternary structure between the CC and CXC family. Several CC chemokine structures form a dimer interface via the formation of a short β-strand along the N-terminus, while the CXC chemokines dimerized along the first β-strand. Although this neatly accounted for functional data at the time, evidence that the monomer unit can successfully bind and trigger a receptor coupled with the observation of an increasing number of purely monomeric structures has meant that it is no longer possible to attribute chemokine function to quaternary structure. If monomeric subunits form the active species, then it is desirable to study chemokines that do not associate at concentrations required for functional studies. The structure of HCC-2 (containing three disulfides) was recently determined, and the additional disulfide bond ($Cys^{57}-Cys^{20}$) was shown to have little impact on the structure when it was compared to the structures of other CC chemokines (*44*). In addition, HCC-2 was shown to be monomeric over a wide range of conditions. The three-dimensional structure of I-309 presented in this study is the first example of a chemokine structure in which the helix is anchored to first β-strand through an additional disulfide bridge. We show that I-309 is monomeric, but unlike HCC-2, the additional disulfide bond results in significant structural changes, namely, leading to a disruption of the C-terminal helix and the unique formation of a short β-strand running perpendicular to the plane of the three-stranded β-sheet.

EXPERIMENTAL PROCEDURES

Chemical Synthesis. I-309 was synthesized by stepwise solid phase methods using tBoc protection chemistry. Following hydrogen fluoride deprotection, the polypeptide was folded and purified as previously described (*45*). The purity of the protein was assessed by ion-exchange chromatography and by electrospray mass spectrometry.

NMR Spectroscopy. NMR experiments were performed on a Varian Unity 600 MHz spectrometer at 30 °C. Samples for NMR were 2 mM protein in 90% H_2O/10% ^2H_2O or 99.90% ^2H_2O, containing 20 mM deuterated sodium acetate, 1 mM sodium azide, and 1 mM DSS (pH 5.0). ^1H chemical

shifts were assigned from standard two-dimensional pulse sequences (*46*). Pulse sequences in H_2O incorporated the Watergate sequence to improve water suppression and allow significant reduction in the water presaturation powers used at the beginning of the sequences. A set of NOESY spectra were collected at 50 and 150 ms to identify spin−spin diffusion effects and allow accurate assignment of NOE distances, especially in the determination of side chain rotamers. Overlap of cross-peaks in the two-dimensional spectra and ambiguities in chemical shift assignments were resolved by collection of ^{1}H NMR spectra at 20 and 40 °C and from a natural abundance [^{13}C]HSQC. Spectra were analyzed with NMRView (*47*).

Stereospecific assignments and χ^1 restraints were obtained from the analysis of the $^3J_{\alpha\beta}$ coupling constants in the DQF-COSY spectrum and the relative intensities of the NOEs from the NH and the C_α to C_β protons in a 50 ms NOESY spectrum collected in D_2O. χ^2 torsion angles for leucine residues were obtained from analysis of intraresidue NOEs between the C_α and $C_{\delta1}$ and $C_{\delta2}$ protons after establishing the correct χ^1. A ϕ restraint, corresponding to a specific solution to the Karplus equation, was applied only if it agreed with the purely NOE-driven convergence of the individual ϕ angle in initial structure calculations.

Structural Restraints. $^3J_{HN\alpha}$ coupling constants were measured in a high-resolution DQF-COSY spectrum as described by Kim and Prestegard (*48*). In the initial stages of the calculation, coupling constants of >8.0 Hz or <6.0 Hz were used to determine ϕ angle restraints (*49*). A coupling constant of >8.0 Hz was converted to an angle constraint of $-120 \pm 40°$, and <6.0 Hz was converted to an angle constraint of $-60 \pm 30°$. In the final refinement stages of the structure calculation, the ϕ angle restraints were removed and replaced by direct refinement against the measured backbone coupling constant. ψ angle restraints were determined by analysis of $d_{N\alpha}/d_{\alpha N}$ ratios but only incorporated into the regions of well-defined secondary structure, and typically, large bounds (±100°) were used (*50*). χ^1 angle restraints were determined as described in ref *51*. All structure calculations included the disulfide bonds, Cys^{11}−Cys^{35}, Cys^{12}−Cys^{51}, and Cys^{27}−Cys^{69}, previously determined for I-309 (*6*), and in each case, these were restrained to a distance of 2.02 ± 0.1 Å.

A series of one-dimensional spectra were collected in rapid succession after dissolving I-309 in 99.90% D_2O. Several well-dispersed C_α proton shifts from the core β-sheet region of I-309 could be assigned (residues 29, 44, and 50) from these one-dimensional spectra and were assigned as hydrogen-bonded amide protons. In the structure calculations, these distances were incorporated as an essentially linear restraint where $r_{NH-O} = 1.8-2.4$ Å and $r_{N-O} = 1.8-3.5$ Å and were only added after initial examination of ensembles of structures generated without incorporation of hydrogen bonds.

Structure Calculations. Structures were determined using dynamic simulated annealing protocols of Nilges et al. (*52*) and X-PLOR version 3.851 (*53*). A total of 911 distance restraints were incorporated that were distributed as 272 long-range ($|i - j| > 5$), 127 short-range ($1 < |i - j| < 5$), 222 sequential ($|i - j| = 1$), and 290 intraresidue restraints ($i = j$). In addition, 59 dihedral restraints were employed in the initial stages of the calculations to be replaced by 50 *J*-coupling restraints in the final refinement stage. Initial starting structures were generated from an extended strand and were examined for basic features typical of a chemokine fold. A new starting structure was chosen, and a family of 100 structures were generated. For this round, an extended heating and conformational search stage was still employed (50 ps) to ensure that sufficient conformational space was sampled and the starting structure did not overly bias new structures. In latter rounds, where only minor modifications were made to the input restraints, only the cooling stage of the simulated annealing protocol was employed. Of the family of 100 structures, 40 structures that exhibited the best overall energy, compliance with restraints, and good covalent geometry were selected. The quality of the final families of structures was analyzed using PROCHECK (*54*), MOLMOL (*55*), and VADAR (VADAR-Structural analysis of protein coordinate data. Software available free from http://www.pence.ualberta.ca). For visualization of structures, Insight98 (MSI) was used and the program Molscript (*56*) was used to generate graphical figures.

Table 1: Structural Statistics and Atomic rmsds for a Family of 40 Lowest-Energy I-309 Structures and the Minimized Average Structure

	⟨I-309⟩	I-309_min
all (911)[a]	0.026 ± 0.003	0.015
interresidue (R^{-6} averaged)		
sequential ($\|i - j\| = 1$)	0.026 ± 0.008	0.020
short-range ($2 \le \|i - j\| \le 5$)	0.034 ± 0.003	0.018
long-range ($\|i - j\| \ge 6$)	0.029 ± 0.003	0.013
intraresidue (R^{-6} averaged)		
$i = j$	0.017 ± 0.002	0.015
energies (kcal mol^{-1})[b]		
E_{NOE}	14.12 ± 0.04	10.98
E_{DIHE}	0.589 ± 0.002	1.01
deviations from idealized geometry[c]		
bonds (Å)	0.00321 ± 0.00001	0.0030
angles (deg)	0.5627 ± 0.006	0.537
impropers (deg)	0.3431 ± 0.0002	0.334
atomic rmsd (Å)[d]		
well-ordered regions (residues 25−30 and 39−68)	0.42 ± 0.03	−
backbone atoms (residues 13−68)	0.61 ± 0.09	−
heavy atoms (residues 13−68)	1.16 ± 0.09	−
ϕ and ψ in the Ramachandran plot (%)[e]		
core region	55.8	69.5
additionally allowed regions	37.2	22.9
generously allowed regions	6.2	7.6
forbidden regions	0.9	0

[a] The rmsd of the experimental restraints is calculated with respect to the upper and lower limits of the input restraints for 40 structures (⟨I-309⟩) and the minimized average structure (I-309_min). [b] The values for E_{NOE} and E_{DIHE} are calculated from a square well potential with force constants of 50 kcal mol^{-1} Å^2 and 200 kcal mol^{-1} rad^{-2}, respectively. [c] The values for bonds, angles, and impropers show the deviation from ideal values based on perfect stereochemistry. [d] The rmsd from the average structure. The average structure was obtained by averaging the coordinates of the individual structures. [e] As determined by the program PROCHECK for residues 13−68 (*54*).

RESULTS AND DISCUSSION

Solution Structure of I-309. Assignment of the chemical shifts for protons in I-309 was accomplished using standard two-dimensional sequential assignment techniques. A complete list of these shifts has been deposited in the BioMagResBank (entry 4686). No evidence of dimerization was found during the assignment process, and all assigned

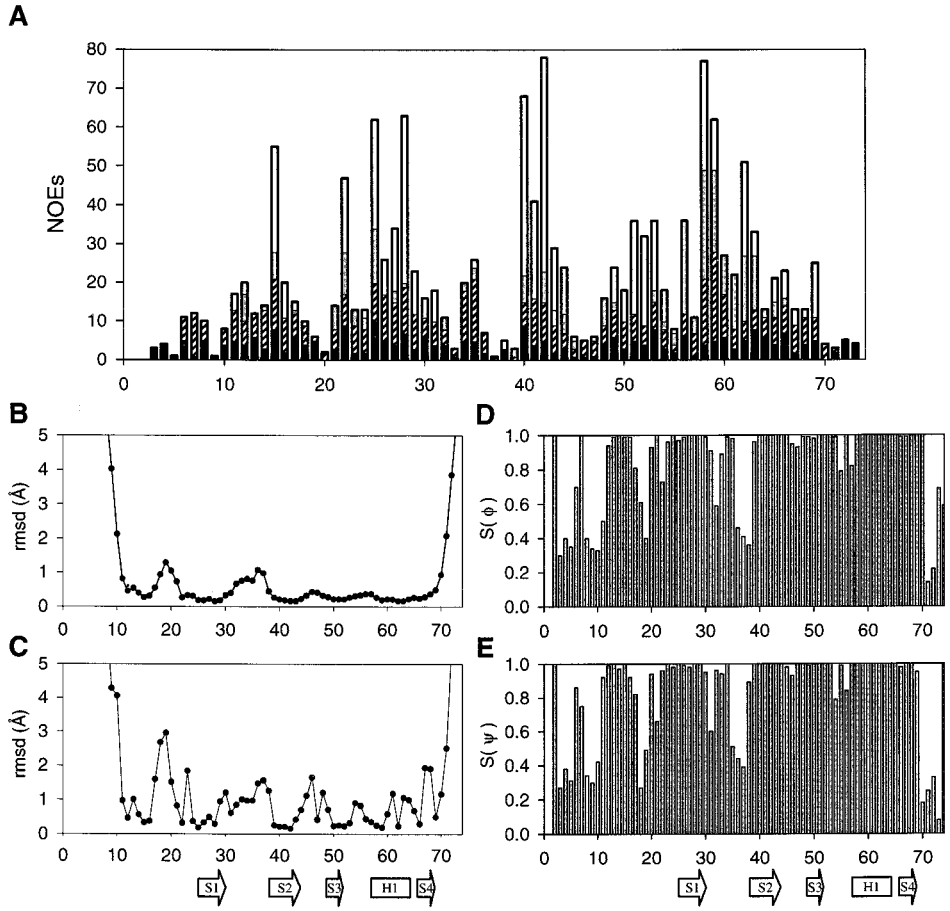

FIGURE 2: Summary of NOE restraints, rmsds, and angular order parameters as a function of residue number for the final 40 I-309 structures. Panel A shows a summary of the number and nature of the NOE restraints per residue vs the amino acid number. The NOEs are represented as follows: intraresidue (black), sequential (stippled), short-range (gray), and long-range (white). Atomic rmsds from the geometric mean structure were calculated (B) for the 40 structures after best fitting the N, C_α, and C backbone atoms of residues 9−68 and (C) for all heavy atoms in the sequence of residues 9−68. Angular order parameters are shown for ϕ (D) and ψ (E).

NOESY cross-peaks were fitted to a monomeric model which was used for structure determination. The calculation of the final 100 I-309 structures, by dynamic simulated annealing using the program X-PLOR (*52*, *53*), was based on a set of 911 NOE distance restraints, 59 dihedral angle restraints, and 8 H-bond restraints. From this set of 100 structures, the 40 energetically most favorable were selected for statistical analysis. All structures in this final family had neither NOE violations of >0.2 Å nor dihedral violations of >2°. The final structures exhibited good covalent geometry as indicated by the low NOE and dihedral energies and the low rmsd from idealized values for bonds, angles, and impropers (Table 1). The negative term for the Lennard-Jones potential, which was approximately −250 kcal mol^{-1}, indicated that the core of the molecule (residues 13−69) was well-packed with few poor nonbonded contacts between atoms. Amino acid residues within this core had an average of 15 NOE restraints (Figure 2A).

Root-mean-square deviations were determined on a residue basis for backbone and heavy atoms (Figure 2B,C). These results showed the N-terminal region (residues 1−10) and the C-terminal region (residues 71−74) to be ill-defined. The only residues within the core of the protein showing rmsds of >1.0 were residues 19, 20, and 36, where the values were 1.29, 1.04, and 1.06, respectively. These results also showed that the region prior to the 3_{10}-helix and the 30s-loop were slightly less well-defined than the remainder of the protein core. The angular order parameter *S* can be used to assess the precision of torsion angles within an ensemble of structures (*57*). This is a statistical parameter that will be equal to 1 if a given torsion angle is identical within a family of structures, while *S* will equal 0 if the angle is undefined. For an *S* near unity, the standard deviation σ (in radians) can be approximated to $S \sim 1 - \sigma^2/2$, giving angular standard deviations of 8°, 18°, and 26° for *S* values of 0.99, 0.98, and 0.9, respectively. The *S* values on a residue basis are shown for ϕ and Ψ angles in panels D and E of Figure 2. Again, the terminal regions, the loop prior to the 3_{10}-helix, and the 30s-loop were the least well-defined.

The family of I-309 solution structures is shown in Figure 3. The structure contained a disordered N-terminus from residues 1 to 10 as seen in other chemokines (*31*, *42*). After the pair of cysteine residues at positions 11 and 12, typically seen in CC chemokines (Figure 1), there was a loop that continued through to residue 21 and a 3_{10}-helix between residues 22 and 24. This was followed by a triple-stranded antiparallel β-sheet. The first strand extended from residue 25 to 30 and the second from residue 39 to 44. Residues in the loop between these strands formed a relatively disordered loop as shown by the rmsds and order parameter (Figure 2). The second and third strands of the β-sheet were connected by a well-defined type I turn, and the third strand extended from residue 49 to 52. A turn connected the third strand of the β-sheet and a C-terminal α-helix. The α-helix was

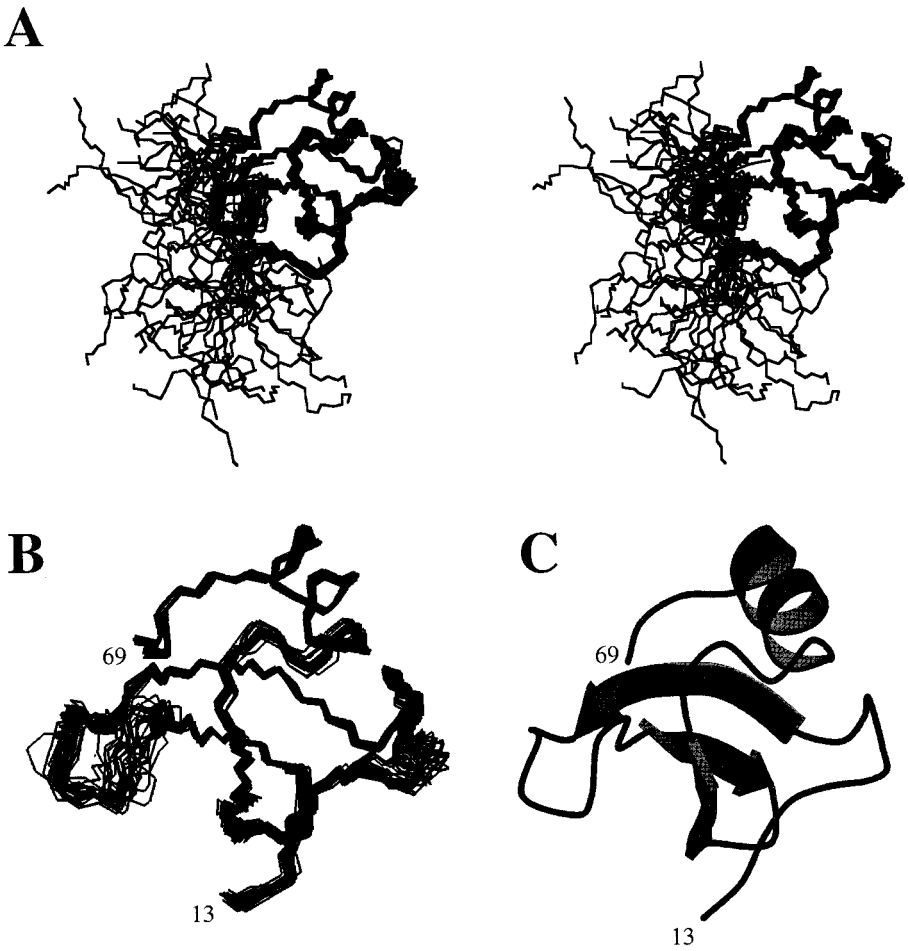

FIGURE 3: Ensemble and average minimized structures of I-309. (A) Superposition of a family of 40 lowest-energy I-309 solution structures showing the disordered N- and C-termini (stereoview). (B) Well-ordered regions of I-309 from residues 13 to 69. (C) A ribbon diagram of the energy-minimized average structure.

disrupted by the third disulfide bond, resulting in the formation of a short extended strand between residues 66 and 69 that is not seen in other chemokines. The remainder of the C-terminus was unstructured.

Comparison to Other CC Chemokines. The three-dimensional structures of the eight CC chemokines determined to date have been highly homologous, with all containing a 3_{10}-helix followed by a triple-stranded antiparallel β-sheet and finally a C-terminal α-helix. It could be predicted that the addition of a third disulfide bond, as present in HCC-2, Ckβ8, and I-309, would result in some distortion of this general structural motif. In the case of HCC-2, the additional disulfide bond was found to have no effect on the overall structure aside from a slight stabilization of the N-terminal amino acid residues between 15 and 20 (*44*). By comparison of the amino acid sequences (Figure 1), it can be seen that a similar situation is likely to exist for Ckβ8. However, while the general protein fold of the I-309 structure conformed to that expected for CC chemokines, significant differences were present at the C-terminus. The α-helix was terminated at residue 65, earlier than observed in all other chemokines, and this was followed by a short extended strand consisting of three residues (Figure 4A). The existence of a strand-like structure was confirmed by ^3J(HN$-$Hα) coupling constants, which were greater than 8 Hz for residues 66$-$68. The biological significance of the extra disulfide bond and resulting extended strand between residues 66 and 68 remains unknown. While it may have implications for the specificity of I-309, it can be seen that the changes do have implications for the ability of I-309 to dimerize along the first β-strand.

Impact of the Third Disulfide Bond. Recently, the solution structure of HCC-2 was determined, and it was shown that the third disulfide bond had no impact on the structure when compared to other known CC chemokine structures such as eotaxin (Figure 4B,C; *42*, *44*). It was proposed that the extra disulfide bond stabilized the orientation of the N-terminal residues 15$-$20 and replaced a normally conserved tryptophan that was not present in HCC-2. However, this is not the case for I-309. Comparison of the amino acid sequences (Figure 1) shows that the position of the extra cysteines is different between chemokines HCC-2 and I-309. In the case of HCC-2, the third disulfide bond was between residue 17 in the first β-strand and residue 57 at the start of the α-helix. However, for I-309 the third disulfide was between residue 27, also in the first β-strand, but to residue 69 and the C-terminal end of the α-helix. This results in the early termination of the α-helix compared to other chemokines and the formation of a short stretch of extended strand between residues 65 and 68 (Figure 4A).

Implications for Dimerization. Many CC and CXC chemokines have been shown to dimerize in solution (*35*, *36*, *39*), and there has been much debate over which is the biologically relevant species: monomer or dimer. Analysis of chemokine structures to date shows that there are two

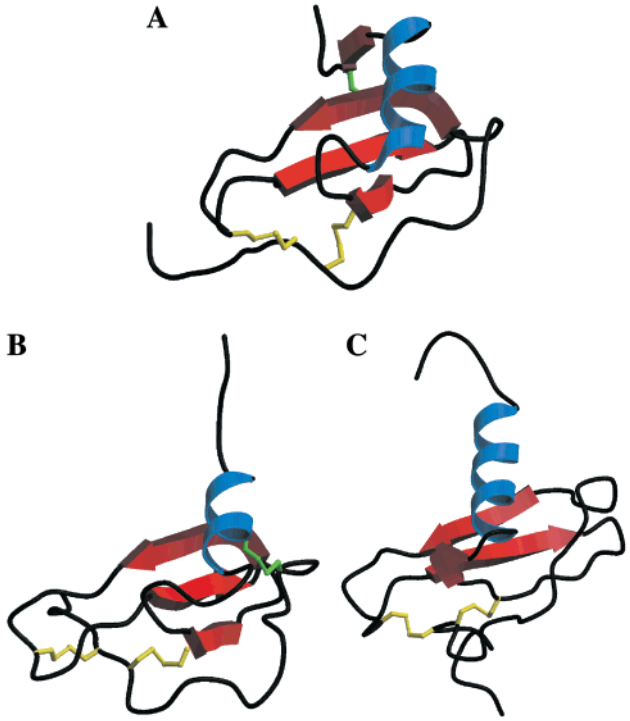

FIGURE 4: Schematic ribbon diagram of (A) I-309, (B) HCC-2, and (C) eotaxin showing regular secondary structure elements. The triple antiparallel β-sheet is shown in red and the α-helix in blue, and random coils are shown in black. Conserved cysteines involved in disulfide bond formation are shown in yellow, while the additional disulfide bond in I-309 and HCC-2 is shown in green.

possible sites where dimerization may occur. The first mode of dimerization, observed in CXC chemokines and the CC chemokine MCP-3 (*39*), is through association along the first β-strand of the two monomer subunits. This results in a compact, six-stranded antiparallel β-sheet that in addition is stabilized by packing against the two C-terminal helices. The second mode of dimerization has only been observed in members of the CC chemokine family. Both MIP-1β and RANTES were found to dimerize via residues in the N-terminal region (prior to the CC motif), resulting in the formation of a short antiparallel β-sheet structure between the two subunits (*35*, *36*).

I-309 was reported not to dimerize up to micromolar concentrations (*7*), and this was confirmed in this study by NMR data at a protein concentration of 2 mM. Most obviously, we were fully able to reconcile all the observed NOEs within a monomeric I-309 model. However, given the limitations of homonuclear NMR methods (e.g., limited spectra resolution), there exits the possibility that intermolecular contacts may have simply been missed. Therefore, other structural data should support our model, and in this instance, evidence is provided by an examination of the N-terminal region and the overall I-309 fold. First, the structural data used in this study are unable to define the N-terminal region. This is typical of the N-termini of several CC chemokines that are observed to be monomeric in solution and where ^{15}N backbone relaxation studies have also shown this region undergoes extensive motion (*62*). It is therefore unlikely that a "CC" type interface is forming along the N-terminal region. Second, the solution structure reveals that the position of the α-helix and C-terminally extended strand that results from the presence of the third disulfide bond blocks the dimerization interface along the first β-strand, preventing the formation of the "CXC" type dimer (Figure 2A).

Our observation that I-309 is monomeric at high concentrations supports the model (*31*, *63*, *64*) that it is the monomeric form of chemokines that forms the biologically active species in vivo. I-309, while a member of the CC chemokine family, has been found to have novel biological functions in apoptosis not shown by other chemokines. It also has the ability to block CCR8-mediated HIV-1 infection. The determination of the three-dimensional solution structure presented in this paper will aid in the understanding of the interactions and specificity of I-309 with its receptor, CCR8.

ACKNOWLEDGMENT

We thank Drs. P. Lavigne, C. McInnes, K. Rajarathnam, and J. Y. Suh for valuable discussions. We acknowledge G. McQuaid for maintenance of NMR spectrometers and Prof. L. E. Kay for pulse sequences. This work was supported by the Protein Engineering Network Centres of Excellence.

REFERENCES

1. Springer, T. A. (1994) *Cell 76*, 301−314.
2. Tashiro, K., Tashiro, K., Tada, H., Heilker, R., Shirozu, M., Nakano, T., and Honjo, T. (1993) *Science 261*, 600−603.
3. Nagasawa, T., Hirota, S., Tachibana, K., Takakura, N., Nishikawa, S.-I., Kitamura, Y., Yoshida, N., Kikutani, H., and Kishimoto, T. (1996) *Nature 382*, 635−638.
4. Baggiolini, M., Dewald, B., and Moser, B. (1994) *Adv. Immunol. 55*, 97−179.
5. Baggiolini, M., Dewald, B., and Moser, B. (1997) *Annu. Rev. Immunol. 15*, 675−705.
6. Paolini, J. F., Willard, D., Consler, T., Luther, M., and Krangel, M. S. (1994) *J. Immunol. 153*, 2704−2717.
7. Patel, V. P., Kreider, B. L., Li, Y., Li, H., Leung, K., Salcedo, T., Nardelli, B., Pippalla, V., Gentz, S., Thotakura, R., Parmelee, D., Gentz, R., and Garotta, G. (1997) *J. Exp. Med. 185*, 1163−1172.
8. Pardigol, A., Forssmann, U., Zucht, H. D., Loetscher, P., Schulz-Knappe, P., Baggiolini, M., Forssmann, W. G., and Magert, H. J. (1998) *Proc. Natl. Acad. Sci. U.S.A. 95*, 6308−6313.
9. Murphy, P. M. (1994) *Annu. Rev. Immunol. 12*, 593−633.
10. Baggiolini, M. (1995) *Clin. Exp. Immunol. 101*, 5−6.
11. Lusti-Narasimhan, M., Chollet, A., Power, C. A., Allet, B., Proudfoot, A. E., and Wells, T. N. C. (1996) *J. Biol. Chem. 271*, 3148−3153.
12. Roos, R. S., Loetscher, M., Legler, D. F., Clark-Lewis, I., Baggiolini, M., and Moser, B. (1997) *J. Biol. Chem. 272*, 17251−17254.
13. Tiffany, H. L., Lautens, L. L., Gao, J., Pease, J., Locati, M., Combadiere, C., Modi, W., Bonner, T. I., and Murphy, P. M. (1997) *J. Exp. Med. 186*, 165−170.
14. Miller, M. D., and Krangel, M. S. (1992) *Proc. Natl. Acad. Sci. U.S.A. 89*, 2950−2954.
15. Bernardini, G., Hedrick, B. G., Sozzani, S., Luini, W., Spinetti, G., Weiss, M., Menon, S., Zlotnik, A., Mantovani, A., Santoni, A., and Napolitano, M. (1998) *Eur. J. Immunol. 28*, 582−588.
16. Garlisi, C. G., Xiao, H., Tian, F., Hedrick, J. A., Billah, M. M., Egan, R. W., and Umland, S. P. (1999) *Eur. J. Immunol. 29*, 3210−3215.
17. Endres, M. J., Garlisi, C. G., Xiao, H., Shan, L., and Hedrick, J. A. (1999) *J. Exp. Med. 189*, 1993−1998.
18. Dairaghi, D. J., Fan, R. A., McMaster, B. E., Hanley, M. R., and Schall, T. J. (1999) *J. Biol. Chem. 274*, 21569−21574.

19. Kledal, T. N., Rosenkilde, M. M., Coulin, F., Simmons, G., Johnsen, A. H., Alouani, S., Power, C. A., Luttichau, H. R., Gerstoft, J., Clapham, P. R., Clark-Lewis, I., Wells, T. N. C., and Schwartz, T. W. (1997) *Science 277*, 1656−1659.
20. Horuk, R., Hesselgesser, J., Zhou, Y., Faulds, Y., Halks-Miller, M., Harvey, S., Taub, D., Samson, M., Parmentier, M., Rucker, J., Doran, B. J., and Doms, R. W. (1998) *J. Biol. Chem. 273*, 386−391.
21. Zhang, X., Chen, L., Bancroft, D. P., Lai, C. K., and Maione, T. E. (1994) *Biochemistry 33*, 8361−8366.
22. Feng, Y., Broder, C. C., Kennedy, P. E., and Berger, E. A. (1996) *Science 272*, 872−877.
23. Doranz, B. J., Rucker, J., Yi, Y., Smyth, R. J., Samson, M., Peiper, S. C., Parmentier, M., Collman, R. G., and Doms, R. W. (1996) *Cell 85*, 1149−1158.
24. Choe, H., Farzan, M., Sun, Y., Sullivan, N., Rollins, B., Ponath, P. D., Wu, L., MacKay, C. R., LaRosa, G., Newman, W., Gerard, N., Gerard, C., and Sodroski, J. (1996) *Cell 85*, 1135−1148.
25. Clore, G. M., Apella, E., Yamada, M., Matsushima, K., and Gronenborn, A. M. (1990) *Biochemistry 29*, 1689−1696.
26. Rajarathnam, K., Clark-Lewis, I., and Sykes, B. D. (1995) *Biochemistry 34*, 12983−12990.
27. St. Charles, R., Walz, D. A., and Edwards, B. F. (1989) *J. Biol. Chem. 264*, 2092−2099.
28. Fairbrother, W. J., Reilly, D., Colby, T. J., Hesselgesser, J., and Horuk, R. (1994) *J. Mol. Biol. 242*, 252−270.
29. Kim, K.-S., Clark-Lewis, I., and Sykes, B. D. (1994) *J. Biol. Chem. 269*, 32909−32915.
30. Hanzawa, H., Haruyama, H., Watanabe, K., and Tsurufuji, S. (1994) *FEBS Lett. 354*, 207−212.
31. Crump, M. P., Gong, J., Loetscher, P., Rajarathnam, K., Amara, A., Arenzana-Seisdedos, F., Virelizier, J., Baggiolini, M., Sykes, B. D., and Clark-Lewis, I. (1997) *EMBO J. 16*, 6996−7007.
32. Dealwis, C., Fernandez, E. J., Thompson, D. A., Simon, R. J., Siani, M. A., and Lolis, E. (1998) *Proc. Natl. Acad. Sci. U.S.A. 95*, 6941−6946.
33. Malkowski, M. G., Wu, J. Y., Lazar, J. B., Johnson, P. H., and Edwards, B. F. (1995) *J. Biol. Chem. 270*, 7077−7087.
34. Shao, W., Jerva, L. F., West, J., Lolis, E., and Schweitzer, B. I. (1998) *Biochemistry 37*, 8303−8313.
35. Lodi, P. J., Garrett, D. S., Kuszewski, J., Tsang, M. L., Weatherbee, J. A., Leonard, W. J., Gronenborn, A. M., and Clore, G. M. (1994) *Science 263*, 1762−1767.
36. Skelton, N. J., Aspiras, F., Ogez, J., and Schall, T. J. (1995) *Biochemistry 34*, 5329−5342.
37. Chung, C., Cooke, R. M., Proudfoot, A. E. I., and Wells, T. N. C. (1995) *Biochemistry 34*, 9307−9314.
38. Kim, K.-S., Rajarathnam, K., Clark-Lewis, I., and Sykes, B. D. (1996) *FEBS Lett. 395*, 277−282.
39. Meunier, S., Bernassau, J., Guillemot, J., Ferrara, P., and Darbon, H. (1997) *Biochemistry 36*, 4412−4422.
40. Handel, T. M., and Domaille, P. J. (1996) *Biochemistry 35*, 6569−6584.
41. Lubkowski, J., Bujacz, G., Boque, L., Domaille, P. J., Handel, T. M., and Wlodawer, A. (1997) *Nat. Struct. Biol. 4*, 64−69.
42. Crump, M. P., Rajarathnam, K., Kim, K., Clark-Lewis, I., and Sykes, B. D. (1998) *J. Biol. Chem. 273*, 22471−22479.
43. Mizoue, S., Bazan, J. F., Johnson, E. C., and Handel, T. M. (1999) *Biochemistry 38*, 1402−1414.
44. Sticht, H., Escher, S. E., Schweimer, K., Forssmann, W. G., Rösch, P., and Adermann, K. (1999) *Biochemistry 38*, 5995−6002.
45. Clark-Lewis, I., Dewald, B., Loetscher, M., Moser, B., and Baggiolini, M. (1994) *J. Biol. Chem. 269*, 16075−16081.
46. Wüthrich, K. (1986) in *NMR of proteins and nucleic acids*, Wiley, New York.
47. Johnson, B. A., and Blevins, R. A. (1994) *J. Biomol. NMR 4*, 603−614.
48. Kim, Y., and Prestegard, J. H. (1989) *J. Magn. Reson. 84*, 9−13.
49. Vuister, G. W., and Bax, A. (1993) *J. Am. Chem. Soc. 115*, 7772−7777.
50. Gagné, S. M., Tsuda, S., Li, M. X., Chandra, M., Smillie, L. B., and Sykes, B. D. (1994) *Protein Sci. 3*, 1961−1974.
51. Wagner, G., Braun, W., Havel, T. F., Schaumann, T., Go, N., and Wüthrich, K. (1987) *J. Mol. Biol. 196*, 611−639.
52. Nilges, M., Clore, G. M., and Gronenborn, A. M. (1988) *FEBS Lett. 229*, 317−324.
53. Brünger, A. T. (1993) in *X-PLOR Version 3.1: A system for X-ray crystallography and NMR*, Yale University Press, New Haven, CT.
54. Laskowski, R. A., MacArthur, M. W., Moss, D. S., and Thornton, J. M. (1993) *J. Appl. Crystallogr. 26*, 283−291.
55. Koradi, R., Billeter, M., and Wüthrich, K. (1996) *J. Mol. Graphics 14*, 51−55.
56. Kraulis, P. J. (1991) *J. Appl. Crystallogr. 24*, 946−950.
57. Hyberts, S. G., Goldberg, M. S., Havel, T. F., and Wagner, G. (1992) *Protein Sci. 1*, 736−751.
58. Nilges, M., and O'Donoghu, S. I. (1998) *Prog. Nucl. Magn. Reson. Spectrosc. 32*, 107−139.
59. Sallusto, F., Kremmer, E., Palermo, B., Hoy, A., Ponath, P., Qin, S., Forster, R., Lipp, M., and Lanzavecchia, A. (1999) *Eur. J. Immunol. 29*, 2037−2045.
60. Wilson, S. D., Kucharoo, V. K., Israel, D. I., and Dorf, M. E. (1990) *J. Immunol. 145*, 2745−2750.
61. Wishart, D. S., Boyko, R. F., and Sykes, B. D. (1995) *CABIOS, Comput. Appl. Biosci. 10*, 687−688.
62. Crump, M., Spyracopolous, L., Lavigne, P., Kim, K.-S., Clark-Lewis, I., and Sykes, B. D. (1999) *Protein Sci. 8*, 2041−2054.
63. Rajarathnam, K., Sykes, B. D., Kay, C. M., Geiser, T., Dewald, B., Baggiolini, M., and Clark-Lewis, I. (1994) *Science 264*, 90−92.
64. Clark-Lewis, I., Kim, K.-S., Rajarathnam, K., Gong, J.-H., Dewald, B., Moser, B., Baggiolini, M., and Sykes, B. D. (1995) *J. Leukocyte Biol. 57*, 703−711.

BI000089L